

Report

Arabidopsis PLETHORA Transcription Factors Control Phyllotaxis

Kalika Prasad,¹ Stephen P. Grigg,^{1,7} Michalis Barkoulas,^{4,7} Ram Kishor Yadav,^{5,7} Gabino F. Sanchez-Perez,^{2,6} Violaine Pinon,¹ Ikram Blilou,¹ Hugo Hofhuis,¹ Pankaj Dhonukshe,¹ Carla Galinha,¹ Ari Pekka Mähönen,¹ Wally H. Muller,³ Smita Raman,¹ Arie J. Verkleij,³ Berend Snel,^{2,6} G. Venugopala Reddy,⁵ Miltos Tsiantis,⁴ and Ben Scheres^{1,6,*}

¹Molecular Genetics

²Theoretical Biology and Bioinformatics

³Biomolecular Imaging

Department of Biology, Faculty of Science, Utrecht University, Padualaan 8, 3584 CH Utrecht, The Netherlands

⁴Department of Plant Sciences, Oxford University, South Parks Road, Oxford OX1 3RB, UK

⁵Department of Botany and Plant Sciences, Center for Plant Cell Biology, University of California, Riverside, Riverside, CA 92521, USA

⁶Netherlands Consortium for Systems Biology

Summary

The pattern of plant organ initiation at the shoot apical meristem (SAM), termed phyllotaxis, displays regularities that have long intrigued botanists and mathematicians alike. In the SAM, the central zone (CZ) contains a population of stem cells that replenish the surrounding peripheral zone (PZ), where organs are generated in regular patterns. These patterns differ between species and may change in response to developmental or environmental cues [1]. Expression analysis of auxin efflux facilitators of the PIN-FORMED (PIN) family combined with modeling of auxin transport has indicated that organ initiation is associated with intracellular polarization of PIN proteins and auxin accumulation [2–10]. However, regulators that modulate PIN activity to determine phyllotactic patterns have hitherto been unknown. Here we reveal that three redundantly acting PLETHORA (PLT)-like AP2 domain transcription factors control shoot organ positioning in the model plant *Arabidopsis thaliana*. Loss of PLT3, PLT5, and PLT7 function leads to nonrandom, metastable changes in phyllotaxis. Phyllotactic changes in *plt3plt5plt7* mutants are largely attributable to misregulation of PIN1 and can be recapitulated by reducing PIN1 dosage, revealing that PLT proteins are key regulators of PIN1 activity in control of phyllotaxis.

Results

Structure of the PLETHORA Gene Clade

The *Arabidopsis* euANT clade includes the *AINTEGUMENTA* (ANT) gene, which regulates floral organ lateral growth, and six *AIL/PLT* genes involved in embryogenesis, floral organ growth, and root stem cell maintenance [11–15]. In previous phylogenetic analyses, the PLETHORA (PLT)-like protein

sequences from monocots and eudicots formed separate subclades [16, 17]. We included additional amino acid positions and added further species to the euANT alignment, and we found that within the PLT clade there are exclusively eudicot clusters (PLT1/PLT2 and PLT3/PLT7, the latter also known as AIL7; see Table S1 available online) but that the cluster including PLT5 (also known as AIL5) encompasses both monocot and eudicot sequences (Figure S1A). These results highlight the independent radiation of the *PLT* gene family within eudicot and monocot lineages and indicate that the common ancestor of these groups possessed *PLT5*-like genes. This observation prompted us to investigate the function of *PLT5* in more detail to uncover new and potentially ancestral *PLT* gene functions in flowering plants.

PLT3, PLT5, and PLT7 Control Phyllotaxis

PLT5, along with *PLT3* and *PLT7*, is expressed in shoot tissues, where these genes show distinct but overlapping domains of expression in vegetative and inflorescence shoot apical meristems (SAMs) (Figures 1A–1F; Figures S1C and S1D) [15]. *PLT5* expression was largely uniform within the central zone (CZ) and peripheral zone (PZ) (Figures 1A and 1D; Figure S1D). *PLT3* was expressed in the CZ, and expression was elevated at the sites of primordium inception (Figures 1B and 1E; Figure S1C). *PLT7* expression mostly marked the SAM center (Figures 1C and 1F). All three *PLT* genes were expressed in epidermal and subepidermal layers of the SAM (Figures 1A–1F), and all showed expression in the vasculature of developing leaves (Figures 1A–1C; Figures S1C and S1D). In addition, *PLT5* was expressed throughout the adaxial cells of developing leaves (Figure S1D).

Although *PLT3* contributes to floral organ development [14], the function of *PLT* genes at the SAM has remained unknown. To reveal such a role for *PLTs*, we studied shoot development in *plt3plt5plt7* triple mutants. In wild-type seedlings, the cotyledons and first two leaves emerge in a decussate pattern, where two oppositely positioned organs are generated simultaneously and successive pairs diverge by 90°. Subsequent leaves arise in a spiral pattern, where successive leaves diverge by an angle approximating the so-called “golden angle” of 137.5° (Figure 2A). Strikingly, *plt3plt5plt7* triple mutants delayed this transition from decussate to spiral for two to three leaf pairs (Figure 2B; Figure S2A). Although meristem size across the base was slightly reduced in the mutant, the meristem marker *SHOOT MERISTEMLESS* was expressed as in wild-type (Figures S2B and S2C) [18]. Individual mutant alleles for *PLT3*, *PLT5*, and *PLT7* did not cause any apparent shoot phenotype, but the decussate pattern was maintained in the third and fourth leaves of ~15% of *plt3plt5*, ~30% of *plt3plt7*, and ~60% of *plt3plt5plt7*. Of the opposing leaves three and four in the *plt3plt5plt7* triple mutant, ~80% were equal in size, suggesting their similar developmental age. Later-arising rosette leaves assumed spiral phyllotaxis (data not shown).

The spiral pattern of phyllotaxis in the *Arabidopsis* rosette is maintained through the floral transition (Figure 2C). In *plt3plt5plt7* mutant inflorescences, we observed a clear departure from the spiral pattern of phyllotaxis involving the golden angle. A prominent new pattern revealed successive

⁷These authors contributed equally to this work

*Correspondence: b.scheres@uu.nl

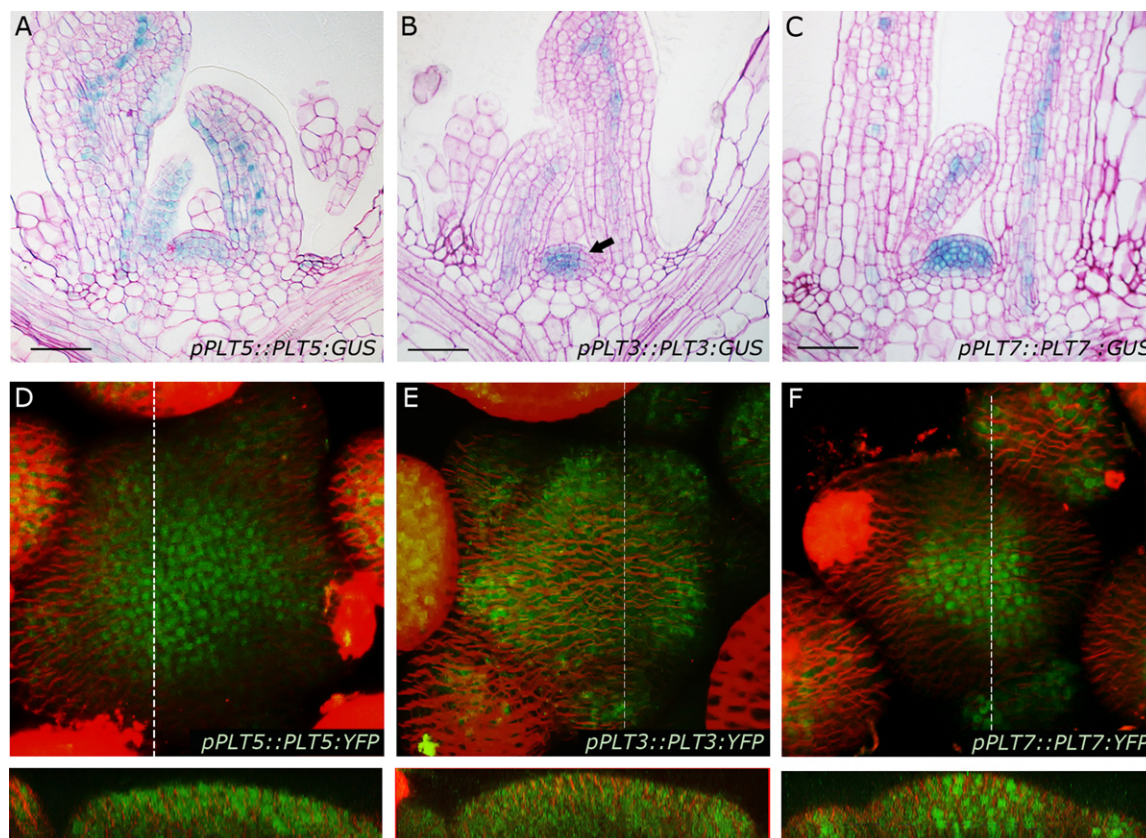


Figure 1. *PLT3*, *PLT5*, and *PLT7* Are Expressed in Overlapping Domains at the Shoot Apical Meristem

(A–C) Median longitudinal sections through vegetative shoot apical meristems (SAMs) expressing *pPLT5::gPLT5::GUS* (A), *pPLT3::gPLT3::GUS* (B), and *pPLT7::gPLT7::GUS* (C). Scale bars represent 50 μ m. Arrow in (B) denotes a region of peripheral zone (PZ) with low expression opposite a region of high expression, as seen in (E) and Figure S1C.

(D–F) Confocal surface projections of wild-type inflorescence meristems (IMs) expressing *pPLT5::gPLT5::YFP* (D), *pPLT3::gPLT3::YFP* (E), and *pPLT7::gPLT7::YFP* (F). Dashed lines in (D–F) denote orientation of the longitudinal optical projections shown in lower panels.

oppositely positioned flowers diverging by 180°; these flowers were either positioned very close to each other or separated along the inflorescence stem (Figure 2D). Another pattern yielded successive flowers diverging by ~90° (Figure 2E). Because these defects could be a result of altered postinitiation growth, we estimated the divergence angle of successive primordia initiating at the SAM by electron microscopy and observed similar divergence angles of ~90° and 180° at the inflorescence meristem (IM) and in mature inflorescences (Figures 2F–2H; Figures S2D–S2G). We concluded that *PLT3*, *PLT5*, and *PLT7* control the positioning of lateral organs at the SAM.

Analysis of divergence angles suggested that the changes in phyllotaxis in *plt3plt5plt7* mutants were highly nonrandom. The triple mutant revealed two new preferred angles, ~90° and 180°, that were not evident in the wild-type or in a *fasciata2* (*fas2*) mutant line [19] that is thought to display random phyllotaxis (Figure 2I). To quantify the nonrandomness of the phyllotactic patterns in *plt3plt5plt7* inflorescences, we calculated the Shannon entropy for the divergence angles [20, 21], which is a measure of the degree of order. The Shannon entropy for wild-type and *plt3plt5plt7* was very similar (2.06 and 2.13, respectively). In contrast, *fas2* showed a higher value (2.54), approaching the maximum entropy (2.77) corresponding to a completely random phyllotaxis. Finally, we compared the relationships between two successive divergence angles in wild-type, *fas2*, and *plt3plt5plt7*. These data revealed

a tendency of *plt3plt5plt7* mutants to divert from the golden angle to ~90° and 180° divergence angles with a new preference for successive 180° angles (Figure 2J), indicating that *PLT3*, *PLT5*, and *PLT7* restrain transitions between specific phyllotactic patterns.

Regulation of PIN1 Abundance by *PLT3*, *PLT5*, and *PLT7* Contributes to Phyllotaxis

In the SAM, polar auxin transport is a major effector of phyllotaxis [2]. We therefore investigated the possibility that *PLTs* in the SAM regulate phyllotaxis through this process, using pharmacological and genetic approaches. First, we found that application of the polar auxin efflux inhibitor *N*-1-naphthylphthalamic acid (NPA) to wild-type plants mimicked the rosette leaf phenotype observed in *plt3plt5plt7* mutants (Figures 3A and 3B; Figures S3A–S3E). Encouraged by this result, we treated weak *plt* mutant combinations (*plt3plt5* and *plt3plt7*) with low concentrations of NPA and monitored the sensitivity by which these mutants revealed phyllotactic changes. Notably, 0.5 or 1.0 μ M NPA did not evoke organ positioning defects in wild-type inflorescences, but ~30% of wild-type seedlings treated with 0.5 μ M NPA switched from spiral to decussate phyllotaxis (Figures 3C and 3D). The frequency of decussate leaves was enhanced in *plt3plt5* and *plt3plt7* up to 80% upon application of 0.5 μ M NPA (Figure 3E). Furthermore, paired flowers appeared in these NPA-treated *plt* mutant

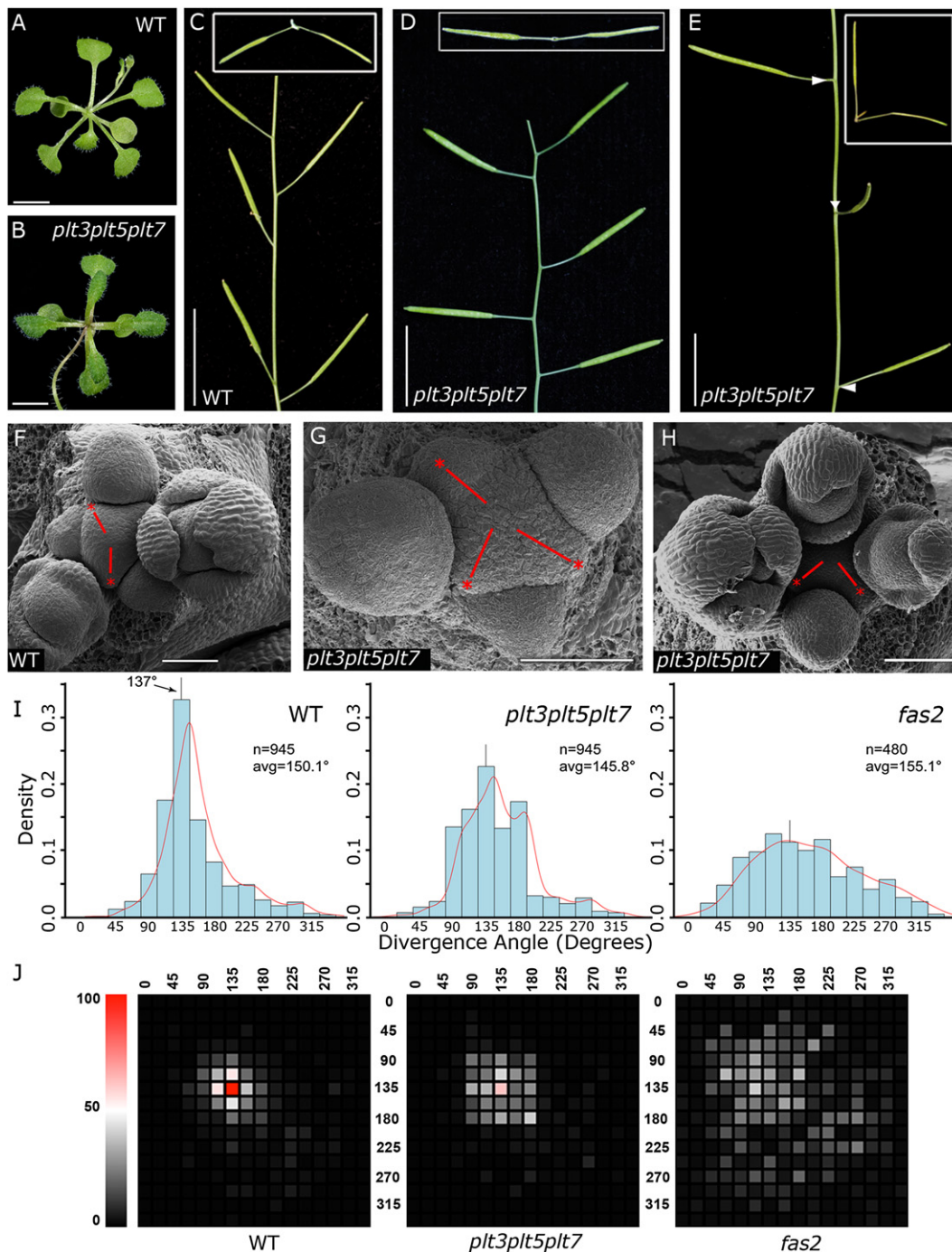


Figure 2. *PLT3*, 5, and 7 Control Phyllotaxis

(A and B) Rosettes of wild-type (WT), with spiral phyllotaxis (A), and *plt3plt5plt7*, with decussate phyllotaxis (B). (C–E) Phyllotaxis patterns in inflorescences of wild-type (C) and *plt3plt5plt7* (D and E). Insets: top views of dissected inflorescences displaying silique divergence angle. (D) Subsequent siliques diverge by 180° . (E) Each silique is positioned nearly perpendicular to the previous silique. (F–H) Scanning electron microscopy (SEM) images of IMs. (F) Wild-type IM showing counterclockwise spiral phyllotaxis. (G and H) *plt3plt5plt7* IMs showing $\sim 90^\circ$ followed by $\sim 180^\circ$ (G) and $\sim 90^\circ$ (H) divergence angles. Lines approximate the trajectory from the estimated SAM center to successively initiated primordia (indicated by asterisks). (I) Silique divergence angle distribution in inflorescences of wild-type, *plt3plt5plt7*, and *fas2*; angle classes are defined by their midpoint. (J) Distribution of patterns in successive silique divergence angles from the measurements in (I). For each angle class on the x axis, the occurrence of each class in the following internode, plotted on the y axis, is represented by color intensity with *fas2* intensity scaled 2x for visibility. Scale bars represent 0.5 cm in (A) and (B), 1 cm in (C)–(E), and $50\ \mu\text{m}$ in (F)–(H).

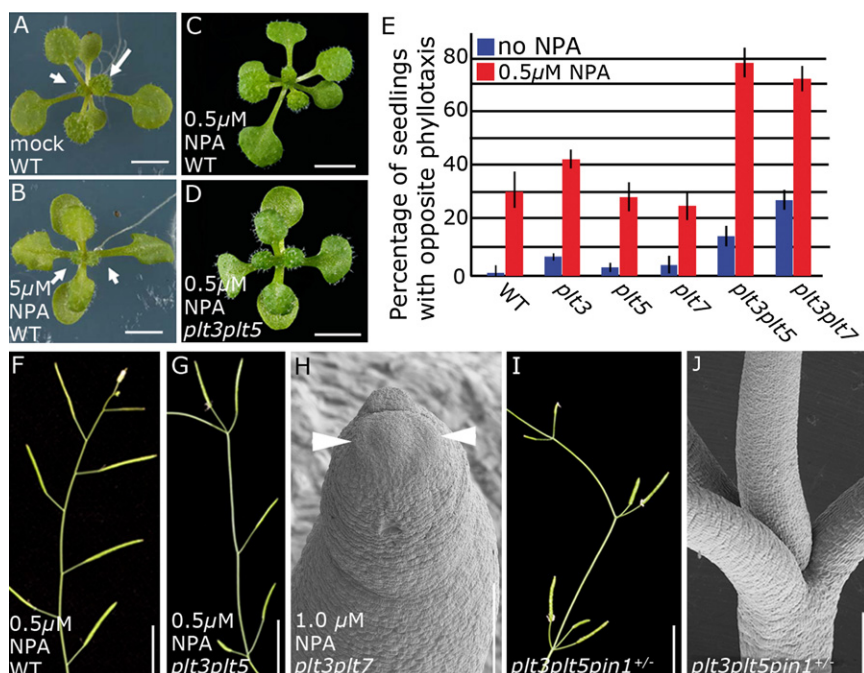


Figure 3. *PLT* Genes and Polar Auxin Transport Synergistically Regulate Shoot Lateral Organ Positioning

(A and B) Wild-type plants grown in the absence (A) or presence (B) of 5 μ M NPA; arrows denote leaves 5 and 6, with arrow length corresponding to leaf length. In (B), these leaves are similar in size and overlap leaves 1 and 2, demonstrating decussate phyllotaxis.

(C and D) Plants grown in the presence of 0.5 μ M NPA: wild-type showing spiral (C) and *plt3plt5* mutant showing decussate phyllotaxis (D).

(E) Quantification of the percentage of wild-type and *plt* seedlings with oppositely positioned second leaf pairs. Error bars represent standard error from three independent experiments.

(F and G) Inflorescences of wild-type (F) and *plt3plt5* (G) plants grown with 0.5 μ M NPA, showing paired siliques in (G).

(H) SEM image of a partially naked inflorescence of a *plt3plt7* plant grown with 1 μ M NPA. Arrowheads indicate floral primordia arising oppositely.

(I) *plt3plt5pin1+/-* inflorescence showing two and three siliques at the same node.

(J) SEM image of the lower node in (I).

combinations (Figures 3F and 3G). Moreover, application of 1.0 μ M NPA promoted the emergence of naked *pin1*-like inflorescences in *plt3plt5* and *plt3plt7* mutants without affecting wild-type inflorescences (Figure 3H; Figure S3F). Notably, genetic reduction of *PIN1* dosage in *plt3plt5pin1+/-* or *plt3plt7pin1+/-* plants also enhanced phyllotactic defects such as the near simultaneous production of flowers from the same node (Figures 3I and 3J).

Our results suggested that *PLT* genes could regulate *PIN1* activity in the shoot; therefore, we analyzed *PIN1*:GFP localization in the SAM of *plt3plt5plt7* mutants. We observed that, rather than forming discrete foci of high expression at incipient primordia as in wild-type, *PIN1*:GFP accumulated more evenly throughout the PZ of *plt3plt5plt7* mutant SAMs with less pronounced foci of *PIN1*:GFP induction (Figures 4A and 4B; Figure S4A; data not shown). We concluded that the corresponding *PLT* proteins are required for increasing *PIN1* levels at shoot lateral organ primordia under circumstances where a base level of *PIN1* expression is sufficient to drive organ initiation. Furthermore, *PLT5*:GR (*PLT5* fused to the rat glucocorticoid receptor [22]) induction elevated *PIN1* transcripts within 4 hr (Figure 4C), suggesting that *PIN1* is regulated by *PLTs* at least in part at the transcriptional level.

If lowering *PIN1* level is a contributing factor to phyllotactic perturbations in *plt* mutant combinations, *PIN1* reduction alone should be sufficient to alter the phyllotactic pattern. Such an effect might be masked by the fusion and outgrowth defects of previously described *pin1* mutants [2, 3]. To further investigate a possible role for *PIN1* dosage in control of phyllotaxis, we reduced *PIN1* expression via RNA interference (RNAi). Strikingly, moderately affected *PIN1*-RNAi (*pin1-i*) plants delayed the transition in the rosette from decussate to spiral phyllotaxis (Figure 4D; Figures S4B and S4C).

If *PLT3*, 5, and 7 regulate phyllotaxis mainly through *PIN1* levels, then restoring strong *PIN1* expression to sites of organ initiation in *plt3plt5plt7* mutants should alleviate the requirement for *PLT* activity and shift phyllotaxis toward the wild-type

pattern. We tested this hypothesis by driving *PIN1*:GFP from the *ANT* promoter, which is expressed in incipient primordia in a *PIN1*-independent manner [13, 23]. Indeed, *pANT::PIN1*:GFP;*plt3plt5plt7* plants showed reduced frequency of oppositely positioned second leaf pairs (26 of 144 in *pANT::PIN1*:GFP;*plt3plt5plt7* versus 79 of 151 in *plt3plt5plt7* mutants). In addition, introduction of *pANT::PIN1*:GFP into *plt3plt5plt7* increased the percentage of successive flowers approximating the golden angle and suppressed the enrichment of the $\sim 90^\circ$ and 180° angles characteristic of *plt3plt5plt7*, although a range of additional angles was also observed (Figure 4E). Together, our data show that *PLT*-mediated *PIN1* regulation couples *PLT* activity in the SAM to auxin transport and indicate that this is an important regulatory mechanism controlling phyllotaxis.

Discussion

Previously, the *PLT* gene clade has been implicated in stem cell maintenance, cell division, and growth [11, 12], processes of broad importance in both root and shoot development. The newly emerged patterning roles for *PLT* genes indicate that they also serve to ensure that organ primordia arise at defined positions. Lateral inhibition mechanisms operating between nearby primordia are at the core of many explanations for patterns of phyllotaxis, including those described here (e.g., [24]), and current descriptions of phyllotaxis highlight auxin as a mediator of the lateral inhibition effect. We show here that the acute increase in *PIN1* accumulation characteristic of developing primordia is lost in *plt3plt5plt7* triple mutants, and our rescue experiment causally links changes in *PIN1* levels with altered phyllotaxis. Furthermore, lowering *PIN1* transcript level is in itself sufficient to change phyllotaxis in *Arabidopsis*, consistent with earlier experiments in other plant species reporting phyllotactic switches upon inhibition of polar auxin transport [25–27]. Taken together, our data suggest that *PLT* gene function controls an

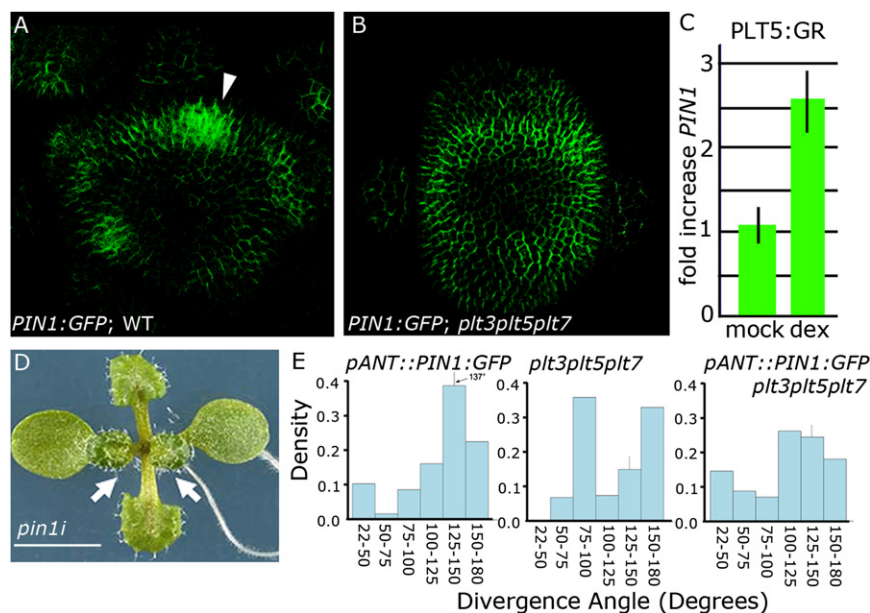


Figure 4. *PLT* Genes Regulate Phyllotaxis through *PIN1* Expression Levels

(A and B) Confocal projections showing *PIN1:GFP* localization in wild-type (A) and *plt3plt5plt7* (B) IMs; arrowhead indicates position of an incipient primordia as inferred from *PIN:GFP* accumulation.

(C) *PIN1* expression level after 4 hr *PLT5* induction, measured by quantitative RT-PCR. Error bars represent standard error from three independent experiments.

(D) *pin1-i* plant showing decussate phyllotaxis.

(E) Distribution of divergence angles between successive siliques from *pANT::PIN1:GFP*, *plt3plt5plt7*, and *pANT::PIN1:GFP; plt3plt5plt7* inflorescences. *n* = 170 for each genotype.

auxin-based lateral inhibition mechanism through regulation of *PIN1* expression.

Our identification of the *PLT* transcription factors as regulators of phyllotaxis via control of *PIN* transcription lays the groundwork for future studies into control of auxin flux. Further investigation of lateral inhibition mechanisms at the shoot apex will require deduction of auxin accumulation patterns, combined with computation of auxin fluxes based on *PIN* localization, possibly using dynamic imaging [7, 8, 28]. It will be instructive to clarify whether *PLT* gene expression in the shoot is itself controlled by auxin, thus providing a mechanism to “ramp up” *PIN* expression in primordia. Preliminary data indicate that *PLT3* and *PLT5* can be regulated by local auxin addition in a *PIN1*-independent mechanism (K.P. and B.S., unpublished data); therefore, it will be interesting to address whether auxin-mediated *PLT* expression contributes to the organization of phyllotaxis.

Importantly, experiment and theory indicate that central or peripheral zone size or primordium growth can affect phyllotaxis [19, 29–33]. Because *PLT* proteins control both stem cell maintenance and primordium growth, it is possible that phyllotactic alterations observed in *plt* mutants in part reflect altered meristem or primordium size through *PLT* functions. Although we cannot exclude that such size regulation emanates from *PLT* regulation of *PIN* gene expression, a role for growth-related *PLT* target genes seems plausible; the redundant role of many *PLT* and *ANT/AIL* genes in growth and cell division [12–15] might reflect an ancestral function of the eu*ANT* clade in these processes. In addition, *ant plt3* mutants have been shown to affect floral organ positioning, indicating that *ANT* genes can contribute to patterning [14]. Although patterning defects prevail in the *plt3plt5plt7* mutant, there are also noticeable effects on organ outgrowth (K.P., H.H., and B.S., unpublished data). Taking these data together, it appears that growth and patterning functions in the eu*ANT* genes are intertwined. Therefore, analysis of target genes of these transcription factors and of the effects of targets on both growth and patterning will be required to separate these processes and the mechanisms involved. Despite their possible involvement

evolutionary tinkering with these regulators contributed to the striking natural diversity of organ arrangements seen in vascular plants.

Supplemental Information

Supplemental Information includes four figures, two tables, and Supplemental Experimental Procedures and can be found with this article online at [doi:10.1016/j.cub.2011.05.009](https://doi.org/10.1016/j.cub.2011.05.009).

Acknowledgments

K.P. was funded by a long-term European Molecular Biology Organization fellowship and by Netherlands Organisation for Scientific Research (NWO) Spinoza and European Research Council advanced investigator grants. G.F.S.-P. was funded by a CBSG2/NCSB grant. Support from NWO-VENI to P.D., NWO-VIDI to I.B., and a Human Frontier Science Program fellowship to A.P.M. is acknowledged. H.H. was funded by NWO-ALW. Work in M.T.'s laboratory was funded by the Biotechnology and Biological Sciences Research Council (BB/F012934/1), the Gatsby Charitable Foundation, and the Royal Society. Live-imaging data were generated by the Microscopy Core at the Institute for Integrative Genome Biology at the University of California, Riverside and were funded by National Science Foundation grant IOS-0718046 to G.V.R.

Received: February 15, 2011

Revised: April 8, 2011

Accepted: May 5, 2011

Published online: June 23, 2011

References

- Kuhlemeier, C. (2007). Phyllotaxis. *Trends Plant Sci.* 12, 143–150.
- Okada, K., Ueda, J., Komaki, M.K., Bell, C.J., and Shimura, Y. (1991). Requirement of the auxin polar transport system in early stages of Arabidopsis floral bud formation. *Plant Cell* 3, 677–684.
- Galweiler, L., Guan, C., Muller, A., Wisman, E., Mendgen, K., Yephremov, A., and Palme, K. (1998). Regulation of polar auxin transport by AtPIN1 in Arabidopsis vascular tissue. *Science* 282, 2226–2230.
- Reinhardt, D., Mandel, T., and Kuhlemeier, C. (2000). Auxin regulates the initiation and radial position of plant lateral organs. *Plant Cell* 12, 507–518.
- Reinhardt, D., Pesce, E.R., Stieger, P., Mandel, T., Baltensperger, K., Bennett, M., Traas, J., Friml, J., and Kuhlemeier, C. (2003). Regulation of phyllotaxis by polar auxin transport. *Nature* 426, 255–260.

6. Benkova, E., Michniewicz, M., Sauer, M., Teichmann, T., Seifertova, D., Jurgens, G., and Friml, J. (2003). Local, efflux-dependent auxin gradients as a common module for plant organ formation. *Cell* 115, 591–602.
7. Heisler, M.G., Ohno, C., Das, P., Sieber, P., Reddy, G.V., Long, J.A., and Meyerowitz, E.M. (2005). Patterns of auxin transport and gene expression during primordium development revealed by live imaging of the *Arabidopsis* inflorescence meristem. *Curr. Biol.* 15, 1899–1911.
8. de Reuille, P.B., Bohn-Courseau, I., Ljung, K., Morin, H., Carraro, N., Godin, C., and Traas, J. (2006). Computer simulations reveal properties of the cell-cell signaling network at the shoot apex in *Arabidopsis*. *Proc. Natl. Acad. Sci. USA* 103, 1627–1632.
9. Jönsson, H., Heisler, M.G., Shapiro, B.E., Meyerowitz, E.M., and Mjolsness, E. (2006). An auxin-driven polarized transport model for phyllotaxis. *Proc. Natl. Acad. Sci. USA* 103, 1633–1638.
10. Wisniewska, J., Xu, J., Seifertova, D., Brewer, P.B., Ruzicka, K., Blilou, I., Rouquie, D., Benkova, E., Scheres, B., and Friml, J. (2006). Polar PIN localization directs auxin flow in plants. *Science* 312, 883.
11. Aida, M., Beis, D., Heidstra, R., Willemsen, V., Blilou, I., Galinha, C., Nussaume, L., Noh, Y.S., Amasino, R., and Scheres, B. (2004). The PLETHORA genes mediate patterning of the *Arabidopsis* root stem cell niche. *Cell* 119, 109–120.
12. Galinha, C., Hofhuis, H., Luijten, M., Willemsen, V., Blilou, I., Heidstra, R., and Scheres, B. (2007). PLETHORA proteins as dose-dependent master regulators of *Arabidopsis* root development. *Nature* 449, 1053–1057.
13. Elliott, R.C., Betzner, A.S., Huttner, E., Oakes, M.P., Tucker, W.Q., Gerentes, D., Perez, P., and Smyth, D.R. (1996). AINTEGUMENTA, an APETALA2-like gene of *Arabidopsis* with pleiotropic roles in ovule development and floral organ growth. *Plant Cell* 8, 155–168.
14. Krizek, B. (2009). AINTEGUMENTA and AINTEGUMENTA-LIKE6 act redundantly to regulate *Arabidopsis* floral growth and patterning. *Plant Physiol.* 150, 1916–1929.
15. Nole-Wilson, S., Tranby, T.L., and Krizek, B.A. (2005). AINTEGUMENTA-like (AIL) genes are expressed in young tissues and may specify meristematic or division-competent states. *Plant Mol. Biol.* 57, 613–628.
16. Kim, S., Soltis, P.S., Wall, K., and Soltis, D.E. (2006). Phylogeny and domain evolution in the APETALA2-like gene family. *Mol. Biol. Evol.* 23, 107–120.
17. Floyd, S.K., and Bowman, J.L. (2007). The ancestral developmental tool kit of land plants. *Int. J. Plant Sci.* 168, 1–35.
18. Long, J.A., Moan, E.I., Medford, J.I., and Barton, M.K. (1996). A member of the KNOTTED class of homeodomain proteins encoded by the STM gene of *Arabidopsis*. *Nature* 379, 66–69.
19. Leyser, H.M.O., and Furrer, I.A. (1992). Characterisation of three shoot apical meristem mutants of *Arabidopsis*. *Development* 116, 397–403.
20. Shannon, C.E. (1948). A mathematical theory of communication. *Bell Syst. Tech. J.* 27, 379–423, 623–656.
21. Barabé, D., and Jeune, B. (2006). Complexity and information in regular and random phyllotactic patterns. *Riv. Biol.* 99, 817–829.
22. Aoyama, T., and Chua, N.H. (1997). A glucocorticoid-mediated transcriptional induction system in transgenic plants. *Plant J.* 11, 605–612.
23. Kuhlemeier, C., and Reinhardt, D. (2001). Auxin and phyllotaxis. *Trends Plant Sci.* 6, 187–189.
24. Douady, S., and Couder, Y. (1996). Phyllotaxis as a dynamical self-organizing process. Part I: The spiral modes resulting from time-periodic iterations. *J. Theor. Biol.* 178, 255–273.
25. Schwabe, W.W. (1971). Chemical modification of phyllotaxis and its implications. *Symp. Soc. Exp. Biol.* 25, 301–322.
26. Meicenheimer, R.D. (1981). Changes in *Epilobium* phyllotaxy induced by N-1-naphthylphthalamic acid and α -4-chlorophenoxyisobutyric acid. *Am. J. Bot.* 68, 1139–1154.
27. Lee, B.H., Johnston, R., Yang, Y., Gallavotti, A., Kojima, M., Travencolo, B.A., Costa, L.F., Sakakibara, H., and Jackson, D. (2009). Studies of aberrant phyllotaxy1 mutants of maize indicate complex interactions between auxin and cytokinin signaling in the shoot apical meristem. *Plant Physiol.* 150, 205–216.
28. Reddy, G.V., Heisler, M.G., Ehrhardt, D.W., and Meyerowitz, E.M. (2004). Real-time lineage analysis reveals oriented cell divisions associated with morphogenesis at the shoot apex of *Arabidopsis thaliana*. *Development* 131, 4225–4237.
29. Douady, S., and Couder, Y. (1996). Phyllotaxis as a dynamical self organizing process. Part II: The spontaneous formation of a periodicity and the coexistence of spiral and whorled patterns. *J. Theor. Biol.* 178, 275–294.
30. Jackson, D., and Hake, S. (1999). Control of phyllotaxy in maize by the *abphyll1* gene. *Development* 126, 315–323.
31. Giulini, A., Wang, J., and Jackson, D. (2004). Control of phyllotaxy by the cytokinin-inducible response regulator homologue ABPHYL1. *Nature* 430, 1031–1034.
32. Goldshmidt, A., Alvarez, J.P., Bowman, J.L., and Eshed, Y. (2008). Signals derived from YABBY gene activities in organ primordia regulate growth and partitioning of *Arabidopsis* shoot apical meristems. *Plant Cell* 20, 1217–1230.
33. Zhao, Z., Andersen, S.U., Ljung, K., Dolezal, K., Miotk, A., Schultheiss, S.J., and Lohmann, J.U. (2010). Hormonal control of the shoot stem-cell niche. *Nature* 465, 1089–1092.